# A New Numerical Analysis of Line Equations Considering Corona Loss on Two-Conductor System

By

Jūrō UMOTO* and Takehisa HARA**

(Received December 23, 1969)

It is very important to investigate the wave attenuation and distortion due to corona discharge, for the purpose of solving successfully the surge problems on the ultra-high voltage transmission systems. So, in this paper, from the nonlinear line equations considering corona loss on a two-conductor system which is expanded from the ones of a single-conductor system, the authors derive a new digital calculation to analyse the attenuation and distortion of the travelling waves caused by corona discharge. Then, they compare their digital computation result under various conditions at the sending end or the receiving end with the experimental ones on the artificial transmission line with other researchers and they make sure that the values of the corona loss constants which have been estimated in the single-conductor system, are adequate values.

## 1. Introduction

The values of the lightning surge voltages on the transmission systems often are higher than the ones of the critical corona voltages of the line conductors, and in such cases the travelling waves are distorted and attenuated due to corona loss. Therefore it is very important to investigate not only the wave distortion and attenuation by the skin effects of the line conductors and the ground return, but also those caused by the corona discharge from the conductor surface, through the line equations.

In this view, the authors have already shown the numerical calculation of attenuation and distortion of the surge on a single conductor due to corona loss and elect the optimum values of the corona loss constants for the surge by comparing the computed results with the experimental ones obtained by Fujitaka and others on a mimic experimental transmission line.

* Department of Electrical Engineering.
** Department of Electrical Engineering, II.

Now, in this paper, we expand the line equations of the single-conductor system to the two-conductor system, and calculate those of the two-conductor system by digital computer with the aid of values of the corona loss constants for surge which have been obtained for the single-conductor system. Next we compare the computed results with the experimental ones obtained by Fujitaka and others on a two-conductor system of a mimic experimental transmission line.

## 2. Numerical Analysis of Line Equations of Two-Conductor System Considering Corona Loss

### 2.1 Line Equations of Two-Conductor System Considering Corona Loss

Already we have given the line equations for single-conductor systems considering corona loss. So, here, let us assume the line equations for two-conductor systems having line voltages exceeding the corona voltage as follows.

$$\left.\begin{aligned}
-\frac{\partial v_1}{\partial x} &= L_{11}\frac{\partial i_1}{\partial t}+L_{12}\frac{\partial i_2}{\partial t},\\
-\frac{\partial v_2}{\partial x} &= L_{21}\frac{\partial i_1}{\partial t}+L_{22}\frac{\partial i_2}{\partial t},\\
-\frac{\partial i_1}{\partial x} &= C_{11}\frac{\partial v_1}{\partial t}+C_{12}\frac{\partial v_2}{\partial t}+\frac{k_1}{v_1}\frac{\partial}{\partial t}(v_1-v_{10})^2+K_1\frac{(v_1-v_{10})^2}{v_1},\\
-\frac{\partial i_2}{\partial x} &= C_{21}\frac{\partial v_1}{\partial t}+C_{22}\frac{\partial v_2}{\partial t}+\frac{k_2}{v_2}\frac{\partial}{\partial t}(v_2-v_{20})^2+K_2\frac{(v_2-v_{20})^2}{v_2},
\end{aligned}\right\} \tag{1}$$

where

$$\left.\begin{aligned}
&v_j \text{ and } i_j\,(j=1,2): \text{ current and voltage of the } j\text{-th conductor at distance } x \text{ from initial point,}\\
&[L]=\begin{bmatrix}L_{11} & L_{12}\\ L_{21} & L_{22}\end{bmatrix}: \text{ inductance matrix of lines per unit length,}\\
&[C]=\begin{bmatrix}C_{11} & C_{12}\\ C_{21} & C_{22}\end{bmatrix}: \text{ capacitance matrix of lines per unit length,}\\
&v_{j0}(j=1,2): \text{ corona voltage of the } j\text{-th line,}\\
&K_j=k_j(f+25)=\sigma_G\sqrt{r_j/2h_j}\times10^{-11}\ (j=1,2)\ [\Omega/m],\\
&k_j=\sigma_C\sqrt{r_j/2h_j}\times10^{-11}\ (j=1,2)\ [F/m],\\
&f: \text{ frequency } [s^{-1}]\\
&r_j \text{ and } h_j\ (j=1,2): \text{ radius and height of the } j\text{-th conductor } [m],\\
&\sigma_G=\sigma_C(f+25),\\
&\sigma_C: \text{ corona loss constant.}
\end{aligned}\right\} \tag{2}$$

In these equations we assume that corona discharge rises only between every conductor and ground, and we neglect the corona discharge between conductors.

Next we consider the problem of seeking the voltage at each point on the line, when the impulse voltage, whose crest value exceeds the corona voltage, is applied on the sending end of the transmission line, whose length is $l$ and which is grounded by the resistance $[z_l]$ at the final end as shown in Fig. 1.

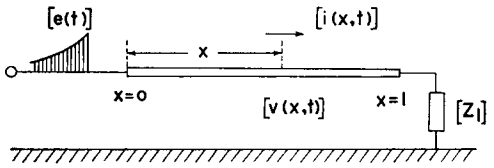

Fig. 1. Two-conductor system.

It is a two boundary value problem namely of solving the nonlinear partial differential Eq.s (1) under the following intial conditions,

$$\left.\begin{aligned}[v(x, 0)] &= [0], \\ [i(x, 0)] &= [0],\end{aligned}\right\} \tag{3}$$

and the boundary conditions,

$$[v(0, t)] = [e(t)], \tag{4}$$

$$[v(l, t)] = [z_l][i(l, t)]. \tag{5}$$

But we should take care that Eq.s (1) are available only if both $v_1$ and $v_2$ are over the corona voltage, and when $v_1$ or $v_2$ is under the corona voltage, we must remove the corona loss terms from Eq.s (1).

The authers have found the three methods of solving such a problem at a single-conductor system. The first and second methods are the ones transforming Eq.s (1) into some approximate linear line equations, and the third method is to solve the non-linear Eq.s (1) as it is. In this paper we shall solve this problem by the third method, which is thought most accurate among the three methods. Moreover, we neglect the surge distortion due to the skin effect in this calculation, because it is very little compared with that of the corona discharge.

## 2.2 Digital Calculating Method of Line Equations

In this section we show the calculating method Eq.s (1) by digital computer. Now, from Eq.s (1) we can introduce the following difference equations concerning $x$ and $t$ after the same procedure as in the case of a single conductor system. Namely, when $i_{1,\nu-1}(t-\Delta t)\neq 0$ or $i_{2,\nu-1}(t-\Delta t)\neq 0$,

$$\left.\begin{bmatrix} i_{1,\nu-1}(t) \\ i_{2,\nu-1}(t) \end{bmatrix} = \begin{bmatrix} i_{1,\nu-1}(t-\Delta t) \\ i_{2,\nu-1}(t-\Delta t) \end{bmatrix} + \begin{bmatrix} L_{11}' & L_{12}' \\ L_{21}' & L_{22}' \end{bmatrix}^{-1} \begin{bmatrix} v_{1,\nu-1}(t)-v_{1,\nu}(t) \\ v_{2,\nu-1}(t)-v_{2,\nu}(t) \end{bmatrix},\right\} \tag{6}$$

when $i_{1,\nu-1}(t-\Delta t)=0$ and $i_{2,\nu-1}(t-\Delta t)=0$,

$$\left.\begin{bmatrix} i_{1,\nu-1}(t) \\ i_{2,\nu-1}(t) \end{bmatrix} = \begin{bmatrix} i_{1,\nu-1}(t-\Delta t) \\ i_{2,\nu-1}(t-\Delta t) \end{bmatrix} + \frac{1}{2}\begin{bmatrix} L_{11}' & L_{12}' \\ L_{21}' & L_{22}' \end{bmatrix}^{-1} \begin{bmatrix} v_{1,\nu-1}(t)-v_{1,\nu}(t) \\ v_{2,\nu-1}(t)-v_{2,\nu}(t) \end{bmatrix},\right\} \tag{7}$$

where

$$
\left.\begin{aligned}
&\nu=1,\ 2,\ \cdots\cdots,\ n,\\
&\begin{bmatrix} L_{11}' & L_{12}' \\ L_{21}' & L_{22}' \end{bmatrix}=\frac{\Delta x}{\Delta t}\begin{bmatrix} L_{11} & L_{12} \\ L_{21} & L_{22} \end{bmatrix},\\
&v_{j\nu},\ i_{j\nu}\ (j=1,\ 2):\ \text{voltage and current of the } \nu\text{-th element of the } j\text{-th conductor},\\
&\Delta x:\ \text{lumped distance of the } \nu\text{-th element},\\
&\Delta t:\ \text{time duration},\\
&n:\ \text{number of total elements}.
\end{aligned}\right\} \tag{8}
$$

Next, from the lower two equations of Eq.s (1), we can arrive at the following equations, when

$$
\left.\begin{aligned}
&\begin{cases} v_{1\nu}(t)<v_{10}, \\ v_{2\nu}(t)<v_{20}, \end{cases}\quad \text{or} \quad \begin{cases} v_{1\nu}(t)<v_{1\nu}(t-\Delta t), \\ v_{2\nu}(t)<v_{2\nu}(t-\Delta t), \end{cases}\\
&\begin{bmatrix} v_{1\nu}(t+\Delta t) \\ v_{2\nu}(t+\Delta t) \end{bmatrix}=\begin{bmatrix} v_{1\nu}(t) \\ v_{2\nu}(t) \end{bmatrix}+\begin{bmatrix} C_{11}' & C_{12}' \\ C_{21}' & C_{22}' \end{bmatrix}^{-1}\begin{bmatrix} i_{1,\nu-1}(t)-i_{1\nu}(t) \\ i_{2,\nu-1}(t)-i_{2\nu}(t) \end{bmatrix},
\end{aligned}\right\} \tag{9}
$$

when

$$
\left.\begin{aligned}
&\begin{cases} v_{1\nu}(t)\geqslant v_{10}, \\ v_{1\nu}(t)\geqslant v_{1\nu}(t-\Delta t), \\ v_{2\nu}(t)<v_{20}, \end{cases}\quad \text{or} \quad \begin{cases} v_{1\nu}(t)\geqslant v_{10}, \\ v_{1\nu}(t)\geqslant v_{1}(t-\Delta t), \\ v_{2\nu}(t)<v_{2\nu}(t-\Delta t), \end{cases}\\
&\begin{bmatrix} v_{1\nu}(t+\Delta t) \\ v_{2\nu}(t+\Delta t) \end{bmatrix}=\begin{bmatrix} v_{1\nu}(t) \\ v_{2\nu}(t) \end{bmatrix}+\begin{bmatrix} C_{11}'+2k_1'(1-v_{10}/v_{1\nu}(t)) & C_{12}' \\ C_{21}' & C_{22}' \end{bmatrix}^{-1}\\
&\quad\times\begin{bmatrix} i_{1,\nu-1}(t)-i_{1\nu}(t)-K_1\Delta x(v_{1\nu}(t)-2v_{10}+v_{10}^2/v_{1\nu}(t)) \\ i_{2,\nu-1}(t)-i_{2\nu}(t) \end{bmatrix},
\end{aligned}\right\} \tag{10}
$$

when

$$
\left.\begin{aligned}
&\begin{cases} v_{1\nu}(t)<v_{10}, \\ v_{2\nu}(t)\geqslant v_{20}, \\ v_{2\nu}(t)\geqslant v_{2\nu}(t-\Delta t), \end{cases}\quad \text{or} \quad \begin{cases} v_{1\nu}(t)<v_{1\nu}(t-\Delta t), \\ v_{2\nu}(t)\geqslant v_{20}, \\ v_{2\nu}(t)\geqslant v_{2\nu}(t-\Delta t), \end{cases}\\
&\begin{bmatrix} v_{1\nu}(t+\Delta t) \\ v_{2\nu}(t+\Delta t) \end{bmatrix}=\begin{bmatrix} v_{1\nu}(t) \\ v_{2\nu}(t) \end{bmatrix}+\begin{bmatrix} C_{11}' & C_{12}' \\ C_{21}' & C_{22}'+2k_2'(1-v_{2\nu}/v_{20}(t)) \end{bmatrix}\\
&\quad\times\begin{bmatrix} i_{1,\nu-1}(t)-i_{1\nu}(t) \\ i_{2,\nu-1}(t)-i_{2\nu}(t)-K_2\Delta x(v_{2\nu}(t)-2v_{20}+v_{20}^2/v_{2\nu}(t)) \end{bmatrix},
\end{aligned}\right\} \tag{11}
$$

when

$$
\left.\begin{aligned}
&v_{1\nu}(t)\geqslant v_{10},\\
&v_{1\nu}(t)\geqslant v_{1\nu}(t-\Delta t),\\
&v_{2\nu}(t)\geqslant v_{20},\\
&v_{2\nu}(t)\geqslant v_{2\nu}(t-\Delta t),
\end{aligned}\right\} \tag{12}
$$

$$\begin{bmatrix} v_{1\nu}(t+\Delta t) \\ v_{2\nu}(t+\Delta t) \end{bmatrix} = \begin{bmatrix} v_{1\nu}(t) \\ v_{2\nu}(t) \end{bmatrix} + \begin{bmatrix} C_{11}'+2k_1'(1-v_{10}/v_{1\nu}(t)) & C_{12} \\ C_{21}' & C_{22}'+2k_2'(1-v_{20}/v_{2\nu}(t)) \end{bmatrix} \times \begin{bmatrix} i_{1,\nu-1}(t)-i_{1\nu}(t)-K_1\Delta x(v_{1\nu}(t)-2v_{10}+v_{10}^2/v_{1\nu}(t)) \\ i_{2,\nu-1}(t)-i_{2\nu}(t)-K_2\Delta x(v_{2\nu}(t)-2v_{20}+v_{20}^2/v_{2\nu}(t)) \end{bmatrix},$$

where

$$\left.\begin{aligned} &\nu=1,\ 2,\ \ldots\ldots,\ n, \\ &\begin{bmatrix} C_{11}' & C_{12}' \\ C_{21}' & C_{22}' \end{bmatrix} = \frac{\Delta x}{\Delta t}\begin{bmatrix} C_{11} & C_{12} \\ C_{21} & C_{22} \end{bmatrix}, \\ &k_j' = \frac{\Delta x}{\Delta t}k_j, \qquad (\mathrm{j}=1,\ 2). \end{aligned}\right\} \tag{13}$$

Using Eq.s (3) to (13), we can calculate the final end voltages according to the following process.

(i) Store the initial values of voltages and currents given by Eq.s (3).

$$[v_\nu(0)] = \begin{cases} [e(0)], & \nu=0, \\ [0], & \nu=1,\ 2,\ \ldots\ldots,\ n, \end{cases}$$
$$[i_\nu(0)] = [0], \qquad \nu=0,\ 1,\ \ldots\ldots,\ n.$$

(ii) Next, calculate the voltages after the time $\Delta t$, namely $[v_\nu(t+\Delta t)]$ ($\nu=1, 2, \cdots\cdots, n$) from Eq.s (9) to (12). On the other hand, we can obtain the values of $[v_0(t+\Delta t)]$ from the boundary condition Eq.s (4), as follows.

$$[v_0(t+\Delta t)] = [e(t+\Delta t)].$$

(iii) Calculate the values of $[i_{\nu-1}(t+\Delta t)]$ ($\nu=1,\ 2,\ \ldots\ldots,\ n$) using the values of $[v_\nu(t+\Delta t)]$ ($\nu=0,\ 1,\ \ldots\ldots,\ n$) which we arrived at (ii), from Eq.s (9) or (10). While, from the boundary condition Eq.s (5), we can compute the values of $[i_n(t+\Delta t)]$ as follows.

$$[i_n(t+\Delta t)] = [z_l]^{-1}[v_n(t+\Delta t)].$$

(iv) After repeating the processes (ii) and (iii) mentioned above, we can get the values of voltages and currents on any point at any time.

## 3. Numerical Calculations and Comparison with the Experimental Results

### 3.1 Numerical Conditions

In this section, the numerical values of the system constants given in the Reference [5] are used in the computations, since we intend to compare the results, which are obtained by the digital computation method described in the previous chapter, with the experimental ones obtained by Asō and Fujitaka. Further we use the values of the corona loss constants $\sigma_C$ and $\sigma_G$ which were obtained in the

single-conductor system.

Table 1. Values of main quantities availed in computation

| | | |
|---|---|---|
| Line lenghth : $l$ | 2067 | [m] |
| Hight of conductors : $h$ | 3.1 | [m] |
| Radius of conductors : $r$ | $1.15\times10^{-3}$ | [m] |
| Lumped distance : $\Delta x$ | 25.8 | [m] |
| Time duration : $\Delta t$ | 0.025 | [$\mu$s] |
| Self surge impedance of line : $z$ | 516 | [$\Omega$] |
| Mutual surge impedance of line : $z'$ | 107 | [$\Omega$] |
| Self inductance of conductor : $L_{11}=L_{22}$ | 1.72 | [$\mu$H] |
| Mutual inducatance of conductor : $L_{12}=L_{21}$ | 0.356 | [$\mu$H] |
| Self capacitance of conductor : $C_{11}=C_{22}$ | 6.72 | [$\mu\mu$F] |
| Mutual capacitance of conductor : $C_{12}=C_{21}$ | $-1.40$ | [$\mu\mu$F] |
| Number of equivalent circuit elements : $n$ | 80 | |

Table 1 shows the values of the constants used in the calculations. And we assume the form of the applied impulse voltage as follows,

$$e(t)=E\exp(-t/\tau), \tag{14}$$

in order to coincide with the experimental one. Then, we perform the numerical calculations of the three sending end conditions corresponding to the experimental ones, namely the case where impulse voltage is impressed on one conductor and the other is grounded at multiple points, the case where voltage is applied to one conductor and the other floats, and the case where voltage is impressed to both conductors simultaneously.

The elements of the voltage matrix in the right side of Eq.(4) vary according to the three sending end conditions as below.

First, when impulse voltage is applied to one conductor and the other is grounded at multiple points, Eq.(4) is expressed as follows.

$$\begin{bmatrix} v_1(0,\ t) \\ v_2(0,\ t) \end{bmatrix}=\begin{bmatrix} e(t) \\ 0 \end{bmatrix}, \tag{15}$$

Next, when voltage is applied to one conductor and the other floats, Eq.(4) becomes

$$\begin{bmatrix} v_1(0,\ t) \\ v_2(0,\ t) \end{bmatrix}=\begin{bmatrix} e(t) \\ z'/z\cdot e(t) \end{bmatrix}, \tag{16}$$

where

$z$ : self surge impedance

$z'$ : mutual surge impedance

Lastly, when voltage is applied to both conductors simultaneously, Eq.(4) is expressed by the following equation.

$$\begin{bmatrix} v_1(0, t) \\ v_2(0, t) \end{bmatrix} = \begin{bmatrix} e(t) \\ e(t) \end{bmatrix}. \tag{17}$$

For the first sending end condition, we give the three kinds of receiving-end conditions where the applied conductor is open-circuited, where it is grounded through matching resistance and where it is grounded through a resister. To the second sending end conditions, we apply the two kinds of receiving end ones where the two conductors are open-circuited and they are grounded through the matching circuit. With respect to the last sending end condition we select the receiving end condition that the two conductors are grounded through the matching circuit.

Now, when the applied conductor is open-circuited at the receiving end, Eq.(5) becomes

$$\left.\begin{aligned} i_1(l, t)&=0, \\ v_2(l, t)&=0. \end{aligned}\right\} \tag{18}$$

When the applied conductor is grounded through matching resistance $z$ at the receiving end, Eq. (5) becomes

$$\left.\begin{aligned} v_1(0, t)&=zi_1(l, t), \\ v_2(l, t)&=0. \end{aligned}\right\} \tag{19}$$

When the applied conductor is grounded through the resistance $R$ at the receiving end, Eq. (5) becomes

$$\left.\begin{aligned} v_1(l, t)&=Ri_1(l, t), \\ v_2(0, t)&=0. \end{aligned}\right\} \tag{20}$$

When the two conductors are open-circuited at the receiving end, Eq. (5) is expressed as

$$\left.\begin{aligned} i_1(l, t)&=0, \\ i_2(l, t)&=0. \end{aligned}\right\} \tag{21}$$

When the two conductors are grounded through the matching circuit at the receiving-end, Eq. (5) is expressed as

$$\begin{bmatrix} v_1(l, t) \\ v_2(l, t) \end{bmatrix} = \begin{bmatrix} z & z' \\ z' & z \end{bmatrix} \begin{bmatrix} i_1(l, t) \\ i_2(l, t) \end{bmatrix}. \tag{22}$$

Next, we will show the calculating method of corona voltage on two-conductor system. The relation between voltages $v_1$ and $v_2$ of two conductors and electric

charges $q_1$ and $q_2$ on the conductors per unit length, is expressed by the following equation.

$$\begin{bmatrix} q_1 \\ q_2 \end{bmatrix} = \begin{bmatrix} C_{11} & C_{12} \\ C_{21} & C_{22} \end{bmatrix} \begin{bmatrix} v_1 \\ v_2 \end{bmatrix}. \tag{23}$$

On the other hand, the surface potential gradient $g$ of the $j$-th conductor is given by

$$g = 9 \times 10^9 \frac{2q_j}{r_j}. \tag{24}$$

Substituting Eq. (24) in Eq. (23), we have

$$\left.\begin{aligned} \frac{10^{-9}}{18} r_1 g &= C_{11}v_1 + C_{12}v_2, \\ \frac{10^{-9}}{18} r_2 g &= C_{21}v_1 + C_{22}v_2. \end{aligned}\right\} \tag{25}$$

As the potential of the $j$-th conductor becomes the corona voltage $v_{j0}$ when its surface potential gradient $g$ rise till the insulation breakdown strength $g_0$ of air, we can arrived at the corona voltage from Eq. (25) as follows.

Since $v_2=0$ when impulse voltage is impressed on one conductor and the other is grounded at many points, we have

$$v_{10} = \frac{10^{-9}}{18} r_1 g_0 / C_{11}. \tag{26}$$

Considering the quality of the conductor surface and the several factors concerning weather, Eq. (26) may be changed as follows.

$$v_{10} = \frac{10^{-9}}{18} m_0 m_1 \delta r_1 g_0 / C_{11} = 27.1 \text{ kV}, \tag{27}$$

where

$m_0$ : surface coefficient of conductor $(=0.96)$,

$m_1$ : weather factor $(=1)$,

$\delta$ : relative density of air $(=1)$,

$g_0$ : insulation breakdown strength of air $(=2.98 \times 10^3 \text{ kV}/m)$.

Since $q_2=0$ when voltage is applied to one conductor and the other floats, we have

$$v_{10} = \frac{10^{-9}}{18} m_0 m_1 \delta r_1 g_0 / \left( C_{11} - \frac{C_{12}^2}{C_{22}} \right) = 28.3 \text{ kV}. \tag{28}$$

Since $v_1=v_2$ and $q_1=q_2$ when voltage is impressed on both conductors, we get the next equation.

$$v_{10} = v_{20} = \frac{10^{-9}}{18} m_0 m_1 \delta r_1 g_0 / (C_{11} + C_{12}) = 34.1 \text{ kV}. \tag{29}$$

### 3.2 Comparison of Calculated and Experimental Examples

In this chapter, the numerical calculations for two-conductor systems are carried

Table 2. Optimum values of $\sigma_C$ and $\sigma_G$ for positive and negative surges

| Wave tail time constants | Positive surge | | Negative surge | |
|---|---|---|---|---|
| | $\sigma_C$ | $\sigma_G$ | $\sigma_C$ | $\sigma_G$ |
| $\tau=5\,\mu s$ | 32 | $20\times10^6$ | 15 | $20\times10^6$ |
| $\tau=20\,\mu s$ | 32 | $16\times10^6$ | 15 | $16\times10^6$ |
| $\tau=80\,\mu s$ | 32 | $30\times10^6$ | 15 | $30\times10^6$ |

out by using the values of $\sigma_C$ and $\sigma_G$ given in Table 2 which were estimated in the single conductor system as shown in the reference [4], and then the calculated waveforms of final end voltages are compared with the experimental ones. Now, in Fig.2~Fig.4 are plotted the digital calculation results of the transient voltages at the receiving end in the case, where at the sending end the impulse voltages are applied to one conductor and at the receiving end it is open-circuited or grounded through matching resistance or 201 $\Omega$-resistor, and the other conductor is grounded at the multiple points. Here the following three kinds of impulse voltages

$$E=\pm230\,\text{kV},\quad \tau=5\,\mu s,$$
$$E=\pm180\,\text{kV},\quad \tau=5\,\mu s,$$
$$E=-80\,\text{kV},\quad \tau=20\,\mu s$$

are used as numerical examples. For comparison, the corresponding experimental

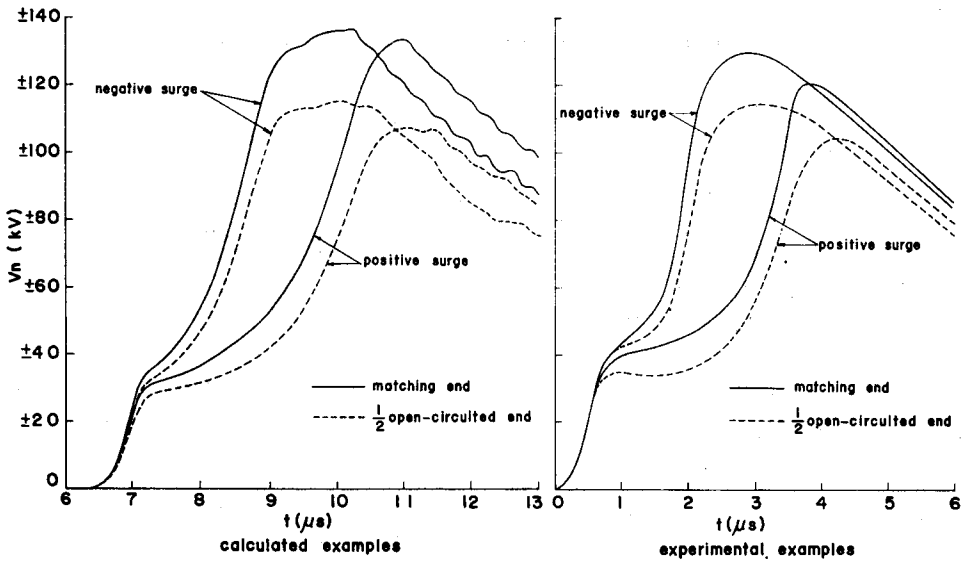


Fig. 2 Receiving end voltage waveforms when the impulse voltages are applied to one conductor and the other is grounded at the multiple points.

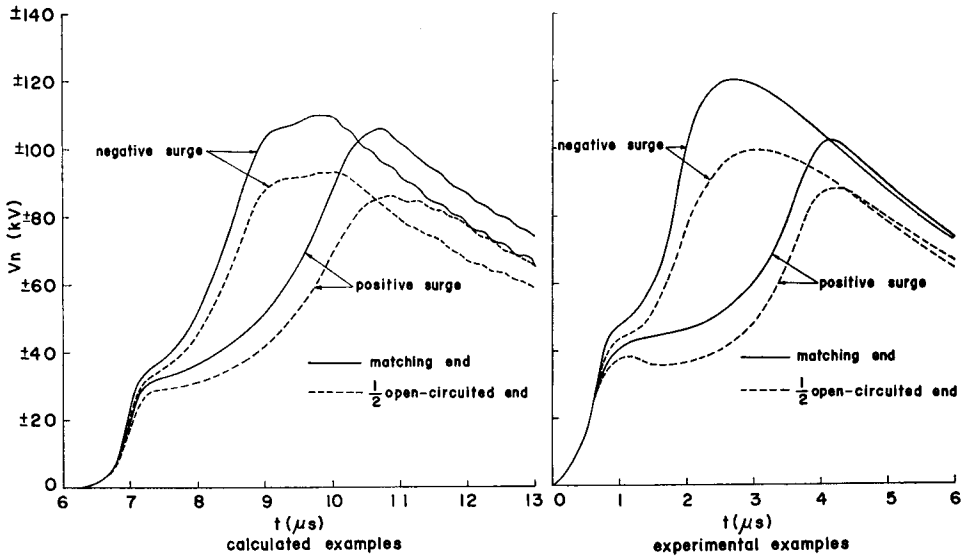


Fig. 3 Receiving end volta e waveforms when the impulse voltages are applied to one conductor and the other is grounded at the multiple points.

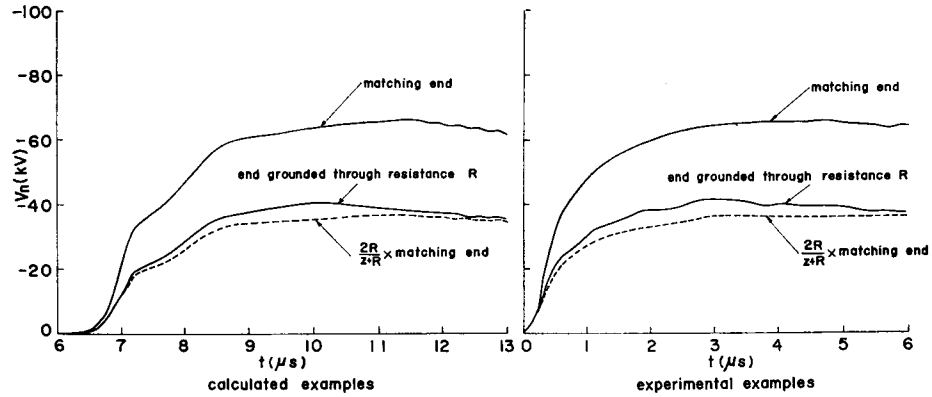


Fig. 4 Receiving end voltage waveforms when the impulse voltages are applied to one conductor and the other is grounded at the multiple points.

waveforms by Asō and Fujitaka are also shown on the right side of the same figures. It will be seen that the attenuation of the peak value and the distortion of the waveform by computation are in good agreement with the experimental ones. Therefore, we can see the value of the corona loss constant $\sigma_C$ and $\sigma_G$ which have been estimated in the single-conductor system are adequate values.

Next Fig. 5 shows the voltage waveforms of the receiving end in the case where voltage is applied on one conductor and the other floats. This time two cases are

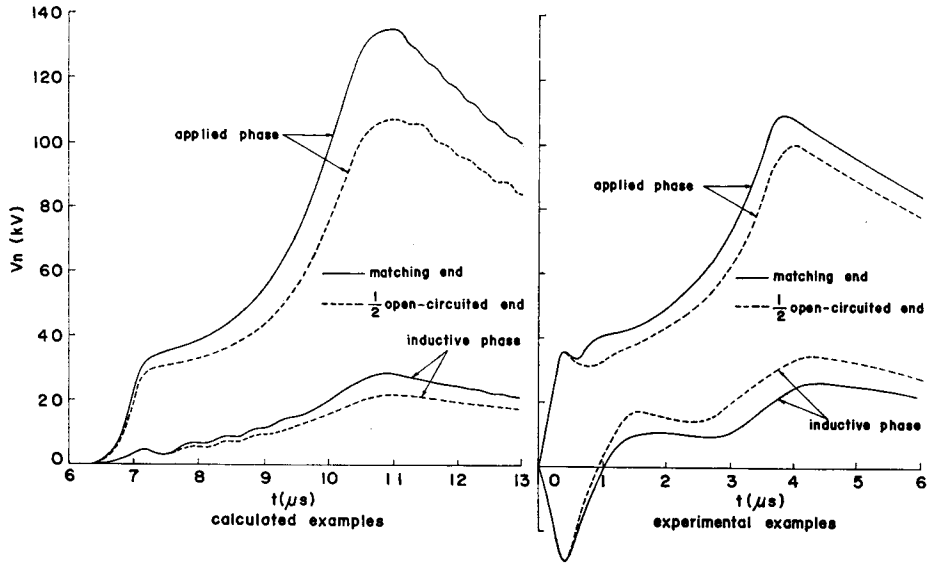


Fig. 5 Receiving end vo age waveforms when the impulse voltages are applied to one conductor and the other is floated.

taken as the two receiving end conditions where the two conductors are matched with surge impedance matrix at the end, and two conductors are open-circuited. And the input impulse voltage is a positive surge namely,

$$E=230\,\text{kV}, \quad \tau=5\,\mu\text{s}.$$

It will be seen that the computed results of the waveforms on the applied conductor show the same tendency as the experimental result. But it is thought unavoidable that the computed waveforms on the other conductor is somewhat different from the experimental ones in the rising portion, since the skin effect is neglected in computation.

Lastly, the waveforms of the receiving end voltages in the case, where the following voltages

$$E=\pm 240\,\text{kV}, \quad \tau=5\,\mu\text{s},$$
$$E=\pm 115\,\text{kV}, \quad \tau=5\,\mu\text{s}$$

are applied to both conductors, which are bound at the sending end and grounded through the matching circuit at the receiving end, are shown in Fig. 6. From the figures we can see that the calculated waveforms differ quantatively a little from the experimental ones, because the latter are considerably distorted by the skin effect, which apears more strongly when the impulse is applied to both conductors simultaneously than when it is applied to only one conductor.

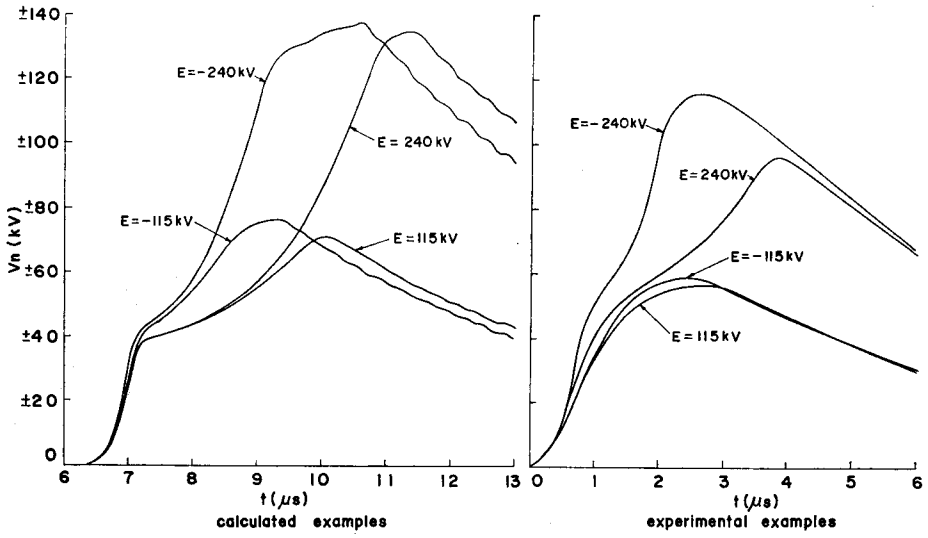


Fig. 6 Receiving end voltage waveforms when the impulse voltages are applied to both conductors simultaneously.

Moreover, from another view of Fig. 2 or Fig. 3, we can see that the open-circuited end voltages rise almost twice that of the matching-end voltages of the sharp wave front below the corona voltage, however, the former end voltages exceeding the corona one are more distorted and attenuated than the latter ones, since, in the former case the corona loss on the conductor increases, as the same polality reflection wave lies upon the incoming wave.

Next, Fig. 4 shows the calculated and experimental data in the case when the conductor is grounded through the resistance, which is about 2/5 of the line surge-impedance, at the receiving end. From this figure, it is made certain that the end voltage exceeds the one, which is calculated with the surge impedance on the contrary above examples, as the corona loss along conductor decreases, because the inverse polality reflection wave lies upon the incoming wave.

## 4. Conclusion

The preceding chapters have been presented a new numerical analysis of the attenuation and distortion of the surges due to corona discharges on a two-conductor system. Furthermore, the practical various computations were carried out by digital computer, and the computed results were compared with the experimental results, which were obtained by Asō and Fujitaka. Since the attenuation of the peak value and the distortion of the waveform by computation are in good agreement with the experimental ones, it was made certain that the values of the corona loss constants

$\sigma_C$ and $\sigma_G$, which had been already estimated in the single-conductor system by the authors, are the adequate values. Moreover, the calculations were carried out concerning various sending end conditions and receiving end conditions. And all these computations were done by FACOM 230-60 in the Kyoto University Computation Center.

Finally, since the range of the crest value and the kinds of the waveforms of the applied voltage used in the computation by the authors are very limited, in order to obtain a more accurate conclusion, it is necessary to perform many additional experiments using other kinds of applied voltages on various line systems. All of these remain for future solutions.

**References**

1) J. Umoto and T. Hara; Convention records at the annual meeting of I.E.E.J., No. 951 (1968).
2) J. Umoto and T. Hara; Memoirs of the Faculty of Engineering, Kyoto University, Vol. XXX, Part 2 Apr. (1968).
3) J. Umoto and T. Hara; Convention records at the annual meeting in Kansai District of I.E.E.J., 1A-2 (1968).
4) J. Umoto and T. Hara; J.I.E.E.J., **89**, 909, May (1969).
5) S. Fujitaka and T. Asō; J.I.E.E.J., **74**, 1211, Oct. (1954).
6) J. Umoto and T. Hara; Convention records at the annual meeting in Kansai District of I.E.E.J., G 4-8 (1969).